The American Association of Petroleum Geologists Bulletin
V. 74, No. 12 (December 1990), P. 1777-1794, 19 Figs., 7 Tables

A Practical Model for Organic Richness from Porosity and Resistivity Logs[1]

Q. R. Passey,[2] S. Creaney,[3] J. B. Kulla,[4] F. J. Moretti,[2] and J. D. Stroud[5]

ABSTRACT

A practical method, the Δ log R technique, for identifying and calculating total organic carbon in organic-rich rocks has been developed using well logs. The method employs the overlaying of a properly scaled porosity log (generally the sonic transit time curve) on a resistivity curve (preferably from a deep-reading tool). In water-saturated, organic-lean rocks, the two curves parallel each other and can be overlain, since both curves respond to variations in formation porosity; however, in either hydrocarbon reservoir rocks or organic-rich non-reservoir rocks, a separation between the curves occurs. Using the gamma-ray curve, reservoir intervals can be identified and eliminated from the analysis. The separation in organic-rich intervals results from two effects: the porosity curve responds to the presence of low-density, low-velocity kerogen, and the resistivity curve responds to the formation fluid. In an immature organic-rich rock, where no hydrocarbons have been generated, the observed curve separation is due solely to the porosity curve response. In mature source rocks, in addition to the porosity curve response, the resistivity increases because of the presence of generated hydrocarbons. The magnitude of the curve separation in non-reservoirs is calibrated to total organic carbon and maturity, and allows for depth profiling of organic richness in the absence of sample data. This method allows organic richness to be accurately assessed in a wide variety of lithologies and maturities using common well logs.

©Copyright 1990. The American Association of Petroleum Geologists. All rights reserved.

[1]Manuscript received, August 18, 1989; revised manuscript received, May 1, 1990; accepted, August 14, 1990.

[2]Exxon Production Research Company, P.O. Box 2189, Houston, Texas 77001.

[3]Esso Resources Canada Ltd., 237 4th Avenue SW, Calgary, Alberta, Canada T2P 0H6.

[4]Exxon Production Research Company, P.O. Box 2189, Houston, Texas 77001. Current address: McLaren Environmental Engineering, 2855 Pullman Street, Santa Ana, California 92705-5713.

[5]Esso Resources Canada Ltd., 237 4th Avenue SW, Calgary, Alberta, Canada T2P 0H6. Current address: Ladeira de S. Pedro, 8300 Silves, Portugal.

We thank Exxon Production Research Company for permission to publish this paper. Also, we are grateful to the various Exxon affiliate offices for approval to use several of the examples. We are grateful to W. A. Young for critical review of early version of this manuscript, and thank J. H. Doveton, S. L. Herron, and I. R. Supernaw for particularly constructive reviews of this manuscript.

INTRODUCTION

Conceptual Model of Organic-Rich Rocks

Source rocks are commonly shales and lime-mudstones that contain significant amounts of organic matter. Non-source rocks also contain organic matter, but the amount is generally not significant (i.e., less than 1 wt. %). The usual method for assessing the richness and maturity of source rocks is through a variety of laboratory analyses (e.g., total organic carbon—TOC—analysis, pyrolysis, elemental analysis, vitrinite reflectance, thermal alteration index, gas chromatography, and visual kerogen description). This paper discusses the effect that organic matter has on the response of common well logging tools, and proposes an easily implemented curve overlay method that is calibrated for organic richness and maturity.

To study the response of well logs in organic-rich rocks, it is necessary to have a conceptual physical model of the material being studied. In the case of a clay-rich rock, the matrix grains are primarily tabular clay minerals, with solid organic matter dispersed among the grains. With increased compaction, the tabular mineral grains tend to align themselves horizontally, with the organic matter distributed in subhorizontal lamellae. From observations of thin sections, the organic matter (primarily kerogen) appears to display ductile behavior. In carbonate source rocks, the primary mineral grains are composed of finely divided calcite and, although the mineral grains often do not have a preferred orientation, these rocks are often laminated with alternating organic-rich and organic-lean layers. It is important to note that the organic matter is originally deposited contemporaneously with the rock matrix grains and does not fill pore voids; perhaps with increased maturation, the kerogen is malleable enough to be squeezed into the pore space, but this should not significantly affect the pore volume in a shale unless the amount of organic matter is relatively high.

For the purpose of this paper, organic-rich rocks are assumed to be composed of three components: (1) the rock matrix, (2) the solid organic matter, and (3) the fluid(s) filling the pore space. Non-source rocks are composed primarily of only two components: the matrix and the fluid filling the pore space (Figure 1A). In immature source rocks, solid organic matter and rock matrix comprise the solid fraction, and formation water fills the pore space (Figure 1B). As the source rock matures, a portion of the solid organic matter is transformed to liquid (or gaseous) hydrocarbons which move into the pore space, displacing

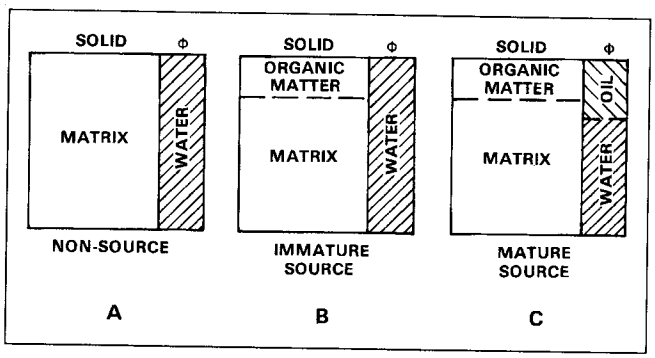

Figure 1—Schematic of solid and fluid components in source and non-source rocks.

the formation water (Figure 1C). This is essentially the model described by Philippi (1968), Nixon (1973), and Meissner (1978), and is the same general model used by Meyer and Nederlof (1984), and Mendelson and Toksoz (1985). The effects of these physical transformations on the porosity and resistivity log responses are the subject of this paper.

Literature Review

Natural Gamma-Ray Logs

Numerous papers have attempted to document the use of well logs for identifying and quantifying source rocks. The physical property used most commonly in identifying organic-rich rocks is that of anomalously high gamma-ray values (Beers, 1945). Where analyses have been made, the anomalous gamma-ray values have been attributed to uranium, associated with the organic matter (Swanson, 1966).

A relationship between total gamma-ray intensity and organic richness has been proposed by Schmoker (1981) for Devonian shales in the Appalachians. Schmoker (1981) noted that the total gamma-ray method significantly underestimates the organic matter in some intervals and that quantitative interpretation of the gamma-ray log in terms of organic matter is not possible across large regions of the Appalachian basin. Thus, extreme care must be exercised in applying this method to evaluate source rock richness in areas outside of the specific Appalachian region where this technique was calibrated.

Recently, the use of gamma-ray spectral logging tools has increased dramatically. Because of the empirically observed relationship between uranium and organic matter (Swanson, 1960), the gamma-ray spectral log has been suggested as a tool that can be used effectively to identify and quantify organic richness (Supernaw et al., 1978; Fertl and Rieke, 1980). Although, at the present time, no universal relationship relating uranium content to organic richness exists, this tool may prove of significant value.

Pulsed-Neutron Spectral Logs

The continuous carbon/oxygen neutron log has had limited application in evaluating TOC content in coals (Rieke et al., 1980; Lawrence et al., 1984) and in organic-rich rocks (Herron, 1986; Herron et al., 1988). The advantages of this tool include the sensitivity to low amounts of organic carbon and that no calibration with core data is required, although corrections for the inorganic carbon content must be made.

Density Logs

Because solid organic matter is less dense than the surrounding rock matrix, Schmoker (1979) proposed the use of the density log for estimating organic matter content. He stated that the density log is more widely applicable and slightly more accurate than the total gamma-ray method; however, because the density log is a pad-type tool and therefore sensitive to borehole rugosity, the usefulness of this tool is decreased in many wells in which the shales are washed out.

In using the density log to determine total organic carbon in the Bakken shale, Schmoker and Hester (1983) noted that because the density log can be significantly affected by the presence of heavy minerals, such as pyrite, a correction for pyrite was necessary based on a linear relationship between pyrite and organic matter.

Gamma-Ray/Sonic Combinations

Dellenbach et al. (1983) developed a method using the transit-time and gamma-ray curves to provide a parameter, I-x, that relates linearly to organic richness. In their method, a source rock is defined by a relatively long transit time (slow velocity) and a high gamma-ray intensity. Even though the derived I-x parameter has been shown in some wells to correlate roughly linearly with organic richness, calibration with sample data from specific wells is required in order to determine organic richness quantitatively.

Another method employing the gamma-ray and transit-time curves was introduced by Autric and Dumesnil (1984, 1985) in which a resistivity parameter is added to the I-x method of Dellenbach et al. (1983). This method involves the selection of a variable which relates to the resistivity in non-source shales. The resistivity curve is used only to help qualitatively discriminate potential source rocks from non-source rocks; the organic richness then is determined using the I-x method (after calibration to sample data).

Resistivity Logs

The response of the resistivity log to organic matter content has received considerably less application, probably because the physical relationships in shale are not well understood. However, the observations by Nixon (1973), Meissner (1978), and Schmoker and Hester (1989) that the resistivity increases dramatically in mature source rocks is an important observation, and presumably is related to the generation of nonconducting hydrocarbons.

Murray (1968) noted that the Bakken shale in the Williston basin often exhibited anomalous readings on the gamma-ray, sonic, neutron, and resistivity logs. Meissner (1978) made several similar observations concerning the log response in the Bakken, among them (1) that the observed high transit time probably results from the high

content of low-velocity organic matter, and (2) that the increased resistivity in the more deeply buried Bakken is related to the onset of maturity and hydrocarbon generation, during which replacement of electrically conductive pore water with non-conductive hydrocarbons takes place; this resistivity curve response has also been discussed by others (Nixon, 1973; Tannenbaum and Aizenshtat, 1985). Meissner (1978) also noted that overpressuring often affects the electrical resistivity of rocks (although the overpressuring was not the cause of the high resistivity anomalies observed in the Bakken), and that the high resistivities observed are opposite to the low resistivities generally associated with high fluid pressures. Although Meissner (1978) did not propose a method to quantify organic richness, he used the resistivity and transit-time curves to map the location of relatively rich and mature source rocks.

Resistivity/Porosity Log Combinations

The use of the resistivity curve for source rock evaluation ranges from the definition of a simple shale resistivity ratio parameter to more complex associations of the resistivity log with porosity and gamma-ray logs (Meyer and Nederlof, 1984; Autric and Dumesnil, 1984, 1985). Also, Smagala et al. (1984) noted that within the Cretaceous Niobrara Formation in the Denver basin, a good relationship exists between maturity (via vitrinite reflectance) and borehole resistivity.

A method involving a combination of resistivity, density, and sonic logs has been introduced by Meyer and Nederlof (1984). The principle behind their method is similar to the method presented here; however, the Meyer and Nederlof (1984) method discriminates between source rocks and non-source rocks without attempting to quantify the organic richness from this combination of logs. Their technique uses either a density/resistivity crossplot, or a transit-time/resistivity crossplot. Data with relatively high resistivity and either relatively high transit time or low bulk density represent a probable source rock; otherwise, the rock is probably barren of organic matter.

Mendelson (1985) and Mendelson and Toksoz (1985) applied multivariate analysis of log data to characterize source rocks. Their study described a physical model to determine log responses relative to source rock properties. It treated the organic matter as a rock constituent and calculated the log responses as a function of organic content. They found that the density, sonic, and neutron logs each respond to the presence of sedimentary organic matter because of its distinctive physical properties. Following the hypothesis of Meissner (1978), they treated the resistivity log as a qualitative maturity indicator, but not as a TOC indicator. Based on single and multivariate regression analysis, various log values are correlated with laboratory measured TOC, and although equations relating log values to measured TOC can be obtained, there are no obvious similarities among any of the multivariate equations; thus the ability to predict TOC in additional wells may be diminished, and the equations derived are location specific and not universally applicable.

Discriminant analysis using a combination of logs proved to be a useful qualitative technique to identify Cretaceous lacustrine source rocks in the Campos basin, offshore Brazil (Abrahao, 1989).

Mann et al. (1986) and Mann and Muller (1988) evaluated the lower Toarcian Posidonia Shale in northern Germany using a combination of spectral natural gamma-ray, bulk density, sonic, and resistivity logs. Good empirical relationships were observed between the logging responses and source richness, hydrocarbon content, and maturity.

Flower (1983) demonstrated a quick-look method to identify possible source rock intervals, in which an induction resistivity curve was overlain on a full-wave sonic (VDL) display. By shifting the resistivity curve so that it coincided with the first shear arrival, the intervals in which coincidence did not occur were interpreted to be possible source rock zones. This method also is similar to the method presented in this paper, but it provides no quantification of organic richness. Another quick-look log overlay technique was recently used by Sinclair (1988) to identify potential source rocks in the Grand Banks area of Newfoundland.

Δ log R TECHNIQUE

Prediction of Organic Richness

The technique presented in this paper was developed and tested within Exxon/Esso beginning in 1979. Since then, it has been successfully applied to many wells worldwide. Although other methods and new tools (such as induced gamma-ray spectral logs) may offer specific advantages in making direct measures of organic carbon content, the technique outlined below has been found to work adequately in both carbonate and clastic source rocks, and can be accurate in predicting TOC over a wide range of maturities (Passey et al., 1989).

Use of Sonic and Resistivity Curves

In applications, the transit-time curve and the resistivity curve are scaled such that their relative scaling is −100 μsec/ft (−328 μsec/m) per two logarithmic resistivity cycles (i.e., a ratio of −50 μsec/ft or −164 μsec/m to one resistivity cycle). The curves are overlain and baselined in a fine-grained, "non-source" rock. A baseline condition exists when the two curves "track" or directly overlie each other over a significant depth range. With the baseline established, organic-rich intervals can be recognized by separation and non-parallelism of the two curves. The separation between them, designated as Δ log R, can be measured at each depth increment. Figure 2 provides a summary of typical scaling and terminology.

The Δ log R separation is linearly related to TOC and is a function of maturity. Using the Δ log R diagram (Figure 3a), the Δ log R separation can be transformed directly to TOC if the maturity (in level of organic metamorphism units, LOM; Hood et al., 1975) can be determined or estimated. In practice, LOM is obtained from a variety of sample analyses (e.g. vitrinite reflectance, thermal alteration index, or T_{max}), or from estimates of burial and thermal history. If the maturity (LOM) is incorrectly estimated, the absolute TOC values will be somewhat in error, but the vertical variability in TOC will be correctly represented. If OMT (organic matter type) is known, then

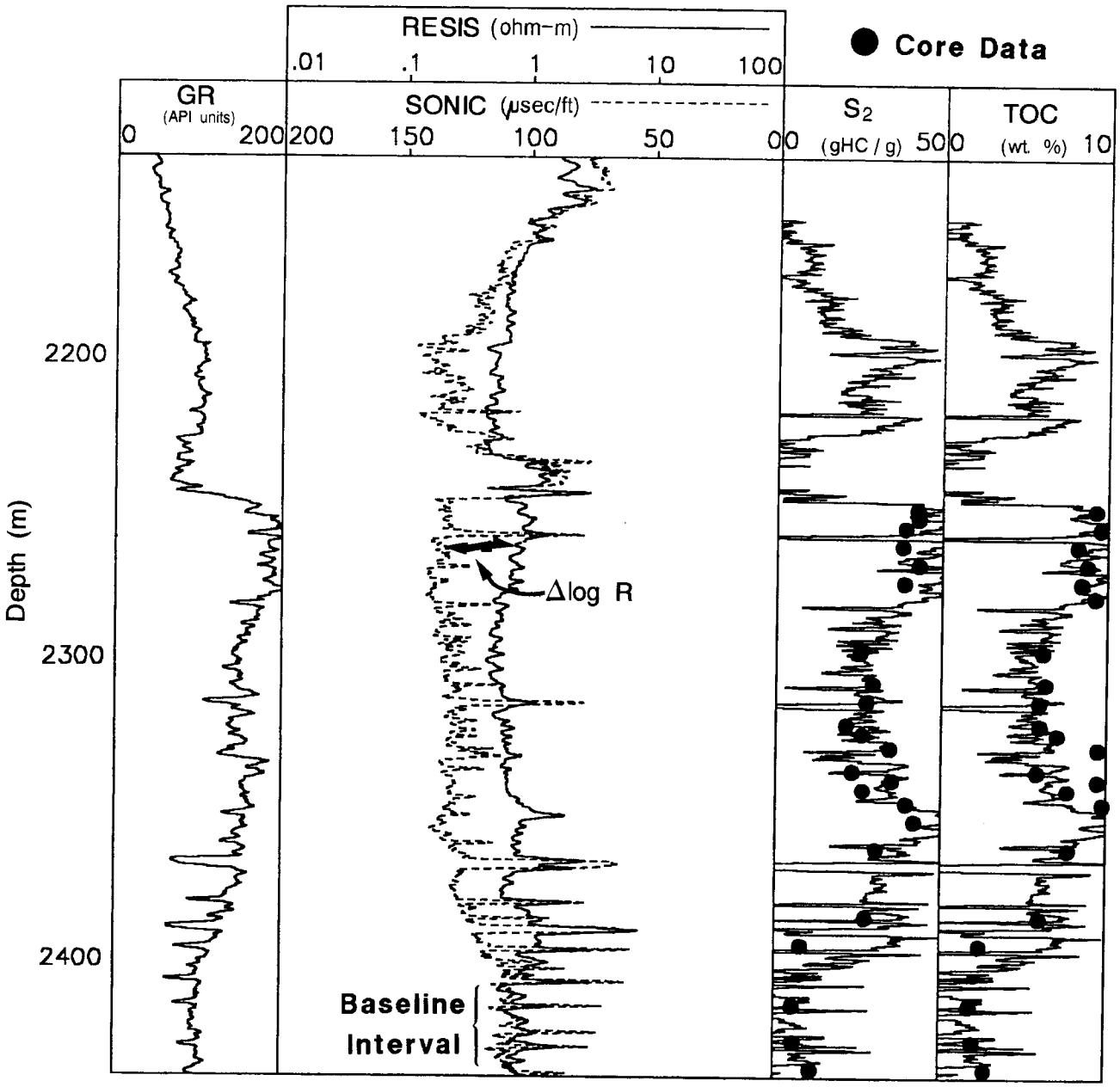

Figure 2—Sonic/resistivity overlay showing Δ log R separation in the organic-rich interval. The relative scaling of the sonic and resistivity curves is 50 μsec/ft (164 μsec/m) corresponds to one decade of resistivity. The values in the center of track 2 correspond to the $R_{baseline}$ and $\Delta t_{baseline}$ values (for this example $R_{baseline}$ = 1 ohm-m, and $\Delta t_{baseline}$ = 100 μsec/ft). This interval is at LOM 6–7 and contains type II kerogen. (LOM = level of organic maturity; Hood et al., 1975.)

pyrolysis S_2 values, as defined by Rock Eval (Espitalie et al., 1977), can be predicted using the transformations of TOC to S_2, as illustrated in Figure 3B, C.

For the example in Figure 2, the maximum Δ log R separation is approximately 0.7 of a logarithmic resistivity cycle (i.e., Δ log R = 0.7), the LOM is 6–7, and the organic matter type (from core) is primarily type II kerogen. Using the Δ log R and LOM values in the diagram (Figure 3A), we calculate the TOC value profile (Figure 2, track 4). Then using the calculated TOC values and the LOM determination of 6–7 in Figure 3B (for type II kerogen), we calculate a profile of S_2 values (Figure 2, track 3). Both the calculated TOC and calculated S_2 values are in good agreement with the measured data from core.

The algebraic expression for the calculation of Δ log R from the sonic/resistivity overlay is

$$\Delta \log R = \log_{10}(R/R_{baseline}) + 0.02 \times (\Delta t - \Delta t_{baseline}) \quad (1)$$

where Δ log R is the curve separation measured in logarithmic resistivity cycles, R is the resistivity measured in ohm-m by the logging tool, Δt is the measured transit time in μsec/ft, $R_{baseline}$ is the resistivity corresponding to the $\Delta t_{baseline}$ value when the curves are baselined in non-

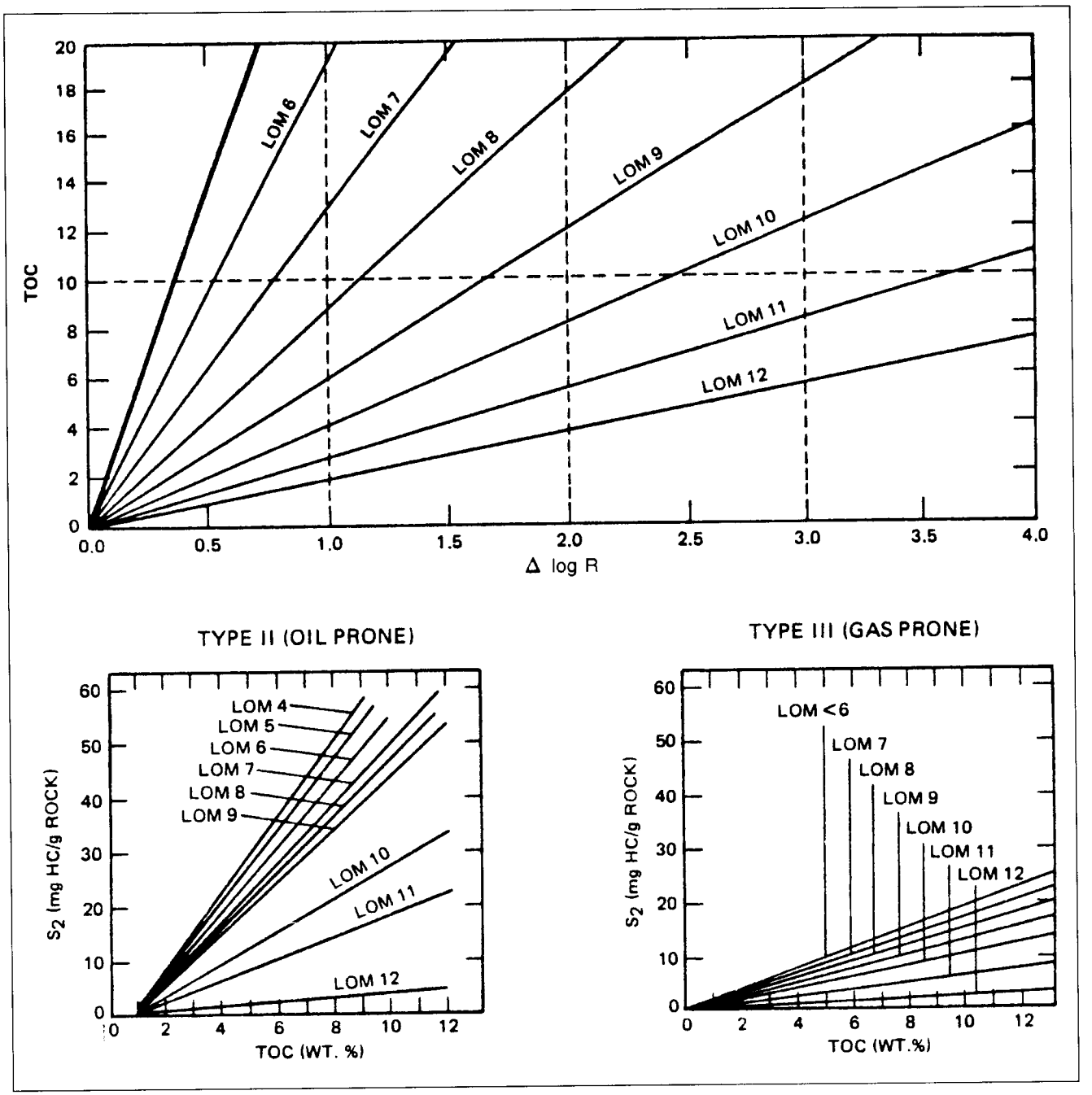

Figure 3—(A) Δ log R diagram relating Δ log R to TOC via maturity. The heavy solid diagonal line near the LOM 6 line should be used for maturity less than LOM 6. (B) TOC to S_2 via maturity diagram for type II (oil-prone) kerogen. This diagram should be used for type I kerogen as well as for type II kerogen. (C) TOC to S_2 via maturity diagram for type III (gas-prone) kerogen.

source, clay-rich rocks, and 0.02 is based on the ratio of −50μsec/ft per one resistivity cycle mentioned above.

Generally, the $\Delta t_{baseline}$ value is constant for an entire well and only the $R_{baseline}$ value is varied in order to overlay or "baseline" the curves. For the interval shown in Figure 2, the curves are plotted using a $\Delta t_{baseline}$ = 100 μsec/ft and a corresponding $R_{baseline}$ = 1.0 ohm-m.

The empirical equation for calculating TOC in clay-rich rocks from Δ log R (Figure 3A) is

$$TOC = (\Delta \log R) \times 10^{(2.297 - 0.1688 \times LOM)} \quad (2)$$

where TOC is the total organic carbon content measured in wt. %, and LOM is the maturity.

An LOM of 7 corresponds to the onset of maturity for oil-prone kerogen, and an LOM of 12 corresponds to the onset of overmaturity for oil-prone kerogen.

Essentially all shales contain some measurable organic carbon. The average TOC in shales worldwide is between

0.2 and 1.65 wt. %; shales generally exceed 0.8 wt. % TOC (Tissot and Welte, 1984). Baselining the transit-time and resistivity curves in non-source, clay-rich rocks implies that the baselined interval is essentially "zero TOC"; in fact, this interval may have approximately 0.8 wt. %. Because of this background TOC, in practice 0.8 wt. % TOC is added to the TOC calculated by equation (2) for all intervals in which positive Δ log R separation occurs, regardless of the magnitude of the Δ log R separation.

A Δ log R separation occurs in both organic-rich source rocks and hydrocarbon-bearing reservoir intervals; thus, a gamma-ray or SP cutoff can be used to eliminate the reservoir intervals when a TOC profile is calculated.

The primary advantage of baselining a porosity curve such as the sonic with a resistivity curve, is that both curves are sensitive to changes in porosity, and once a baseline is established in a given lithology, porosity variations affect the responses of both curves such that a shift in one curve is reflected in a shift of comparable magnitude in the other curve. For example, an increase in porosity results in an increase in Δt, but it also means an increase in the volume of conductive water, resulting in a decrease in resistivity. These changes are proportional, so that if the porosity and resistivity curves are correctly scaled (as described in the Appendix), the amount of increased porosity results in deflections of similar magnitude of both the porosity and resistivity curves; thus, the porosity dependence is removed. This allows for the calculation of TOC in wells for which no direct measurement of TOC exists.

Porosity Log Response to Solid Organic Matter

The three common porosity curves—Δt, bulk density, and neutron porosity—respond to the presence of solid organic matter which has low velocity, low bulk density, and high hydrogen content. All of these attributes produce a response which mimics an increase in porosity. For the well depicted in Figure 2, crossplots of TOC vs. Δt, bulk density, and neutron porosity show linear relationships (Figure 4).

If a suitable transit-time curve is not available, the density or neutron curve can be substituted. These curves also are useful to confirm Δ log R separation observed using the sonic/resistivity curve combination. Use of the density and neutron curves with the resistivity curve to determine TOC is illustrated in Figures 5A, B. Although the determined TOC values (and S_2 values if organic matter type is known) obtained using the density and neutron curves are in fairly good agreement with the measured values, the sonic/resistivity combination has generally been observed to be superior in accuracy to either the density/resistivity or neutron/resistivity combination. This is probably due to the adverse effect of hole conditions on the density and neutron readings.

Empirically derived equations for calculating curve separation when substituting the density or neutron log for the transit-time curve are

$$\Delta \log R_{Neu} = \log_{10} (R/R_{baseline}) + 4.0 \times (\phi N - \phi N_{baseline}) \quad (3)$$

and

$$\Delta \log R_{Den} = \log_{10} (R/R_{baseline}) - 2.50 \times (\rho_b - \rho_{baseline}) \quad (4)$$

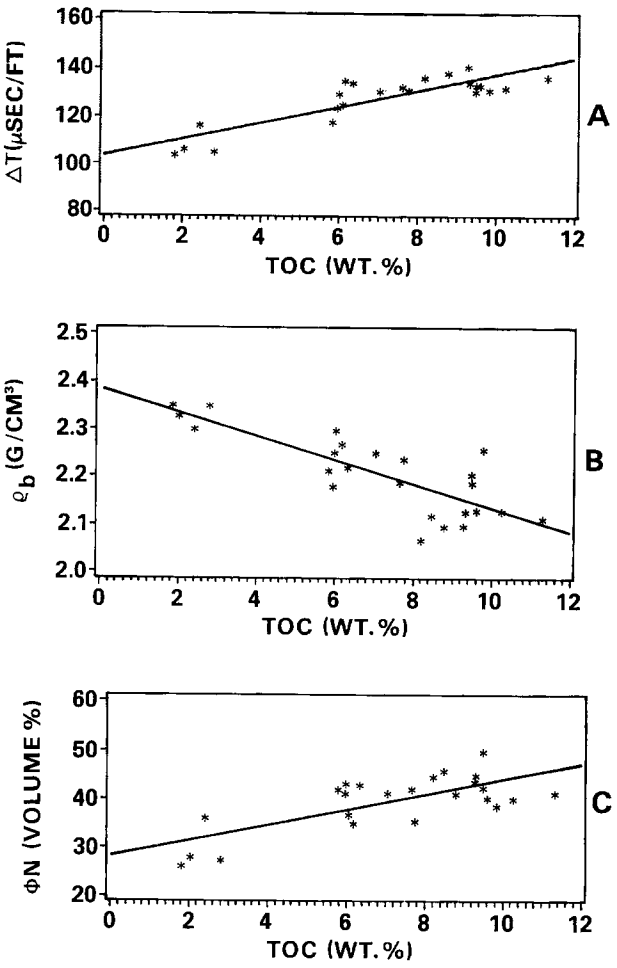

Figure 4—(A) Plot of sonic transit-time vs. measured TOC showing good correlation. These data are listed in Table 2. (B) Plot of bulk density vs. measured TOC. (C) Plot of neutron porosity vs. measured TOC.

where Δ log R_{Neu} and Δ log R_{Den} are Δ log R separations based on the density and neutron logs, respectively, ϕN is the neutron porosity reading from the well log in the interval of interest, $\phi N_{baseline}$ is the neutron porosity baseline value (scaled in fractional porosity), and ρ_b and $\rho_{baseline}$ are the density values for the source rock and baseline intervals, respectively.

As with the sonic curve, a single value for $\phi N_{baseline}$ or $\rho_{baseline}$ generally is used for the entire well, and the baselining with the resistivity curve is achieved by varying only the $R_{baseline}$ value.

The example in Figure 2 is from a relatively immature section; accordingly, the resistivity curve, which responds to the amount and type of formation fluid, shows little change from the organic-lean zone, near the bottom of the section, to the organic-rich zone higher in the section. Due to the response of the porosity curves, however, a Δ log R separation occurs in the organic-rich interval. It can be inferred that the porosity curve (i.e., the transit-time, density, or neutron curve) is responding largely to the amount of solid organic matter; thus, in immature source rocks, sepa-

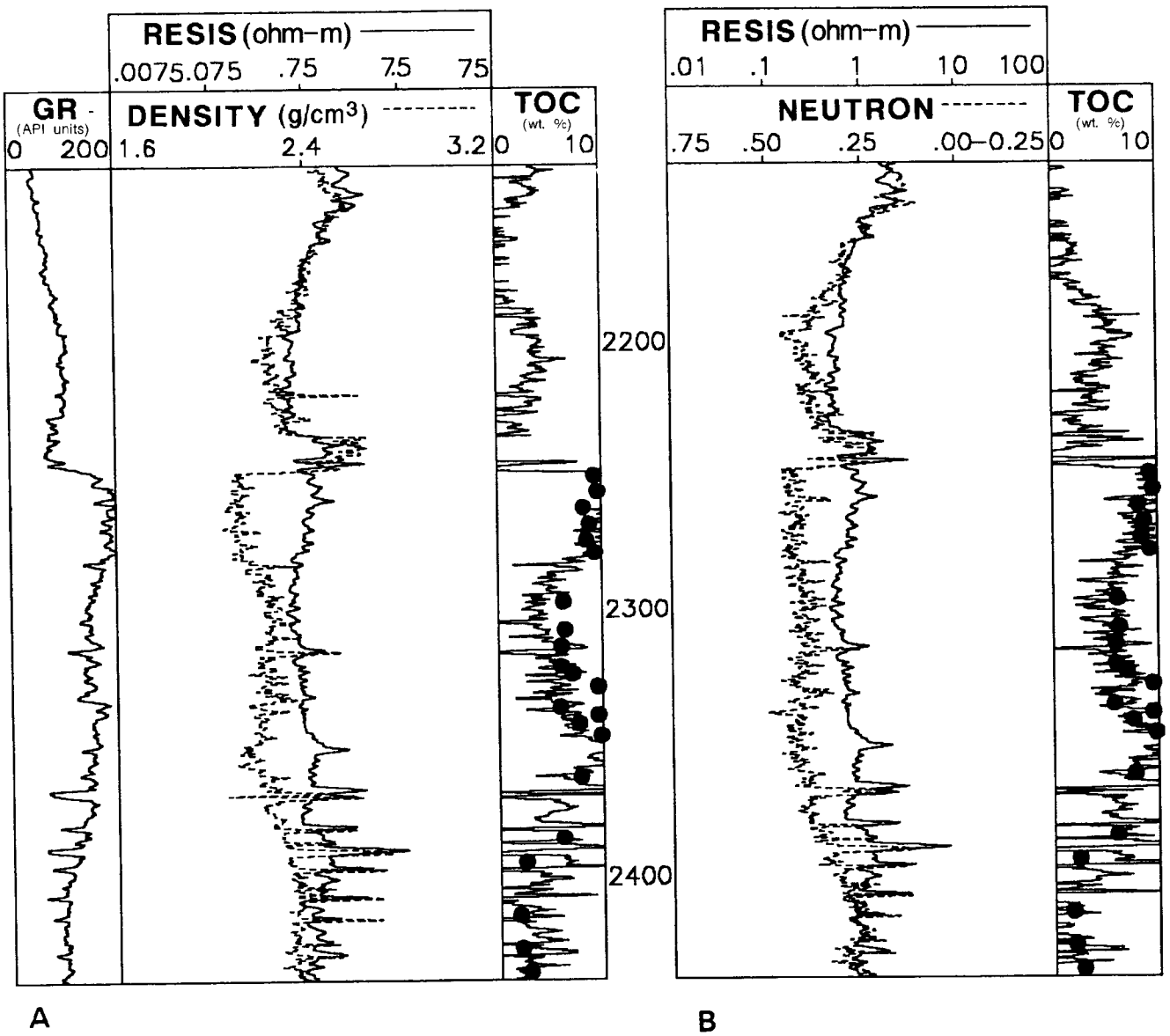

Figure 5—(A) Density (ρ_b)/resistivity overlay and calculated TOC (wt. %) profile. (B) Neutron porosity (ϕ_N)/resistivity overlay and calculated TOC profile. The measured TOC data are from core (indicated by black dots).

ration is caused mainly by movement of the porosity curve to the left, and is largely an expression of organic richness.

Unfortunately, with only a porosity curve to estimate organic richness, it is not possible to distinguish the porosity response from the organic matter response; constant porosity through the analyzed interval must be assumed. Also in order to make quantitative TOC determinations, measured TOC values must be available for calibration; this is essentially how Schmoker (1979) used the density log to determine TOC.

Log Response to Organic Maturity

In addition to the portion of the Δ log R separation caused by porosity curve response to solid organic matter, there is a contribution by the resistivity log response to generated hydrocarbons. Graphic examples of this resistivity curve response are shown in Figure 6. These examples are from the Devonian Duvernay Formation in western Canada. The maturity of well A is approximately LOM 5 (immature); in well B, the maturity is LOM 10.5 (peak maturity). Although similarity exists between the gamma-ray and transit-time curves in these two wells, the resistivity curves are very different. In well A (LOM 5), the resistivity curve is relatively flat across the organic-rich unit, and the Δ log R-derived TOC values result primarily from the response of the transit-time curve. In well B (LOM 10.5), the resistivity curve shows a strong increase in resistivity, responding to generated hydrocarbons. Using the Δ log R/TOC relationship shown in Figure 3A, the Δ log R separation in each well is transformed to TOC values, and these are plotted for each well. Note the similarity between the calculated TOC profiles even though the

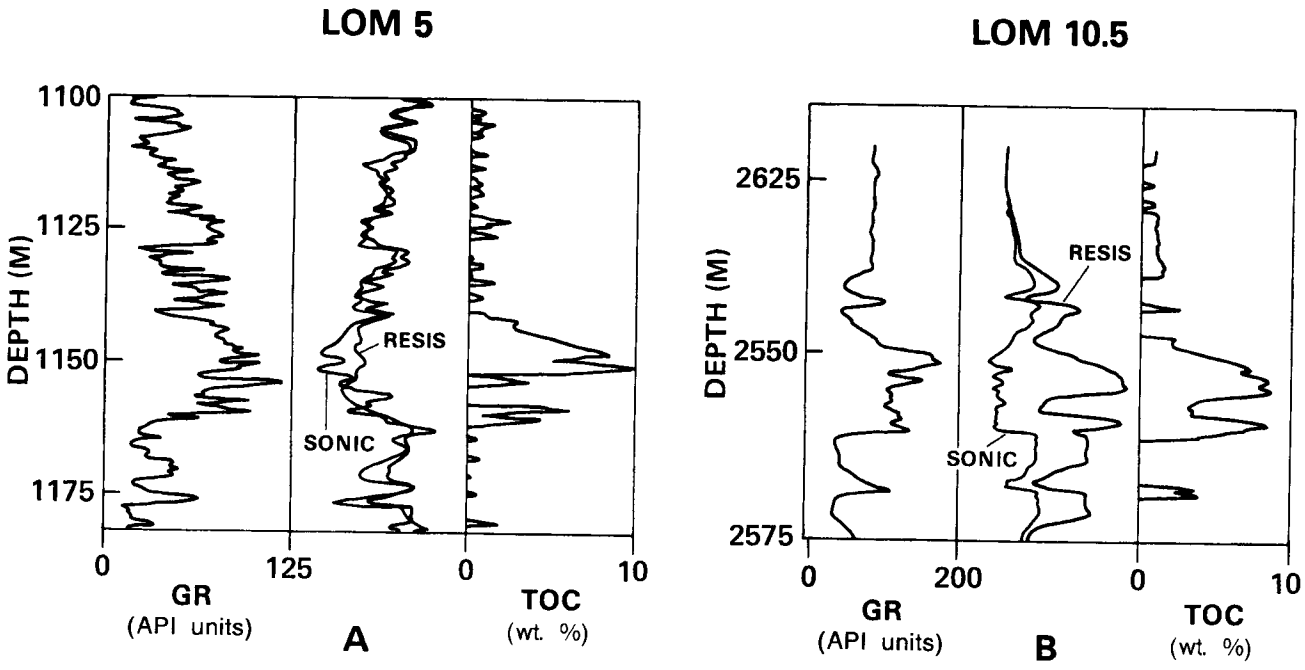

Figure 6—(A) Sonic/resistivity overlay and calculated TOC profile for an immature carbonate source rock in western Canada. (B) Sonic/resistivity overlay and calculated TOC for the same formation at peak maturity. The curves in (B) were hand digitized from a small-scale print; thus, the curves are more smoothed than those in (A).

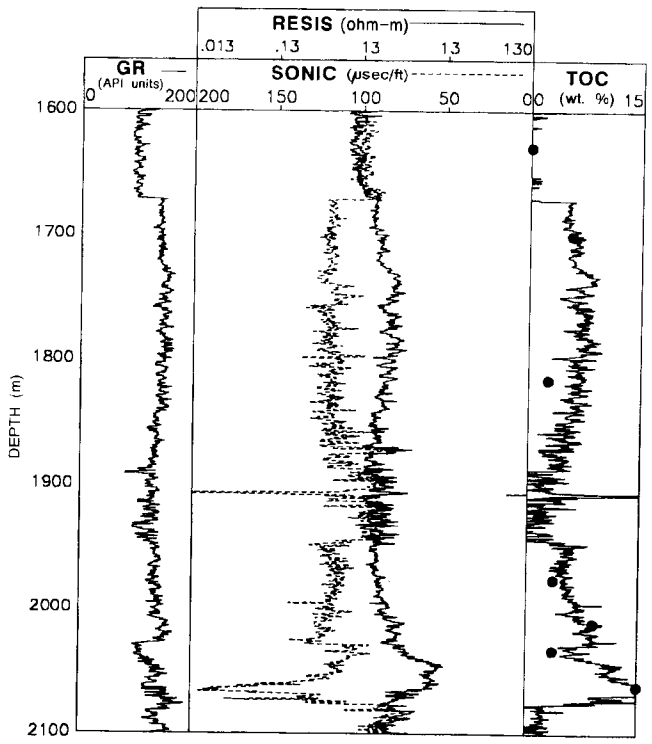

Figure 7—Sonic/resistivity overlay and calculated TOC profile in a lacustrine (type I kerogen) source rock. The measured TOC values are from sidewall cores (black dots).

overlays themselves appear quite different.

Our empirical observation is that the increase in the resistivity response begins at LOM 6–7 for type II (oil-prone) organic matter, suggesting the true onset of maturity for rocks containing type II kerogen. It is possible that under some circumstances, commercial quantities of hydrocarbons may be expelled at these relatively low LOM values (e.g., oils from a Monterey Formation source in California, or in gilsonite veins from Green River shale in Colorado).

In the absence of sample data, the exact maturity cannot be determined from the Δ log R curve-overlay method, although it is possible to determine whether an organic-rich rock is immature or mature (based on the resistivity curve response). If the resistivity curve is relatively flat, the implication is that the interval does not contain any generated hydrocarbons and that the rock is immature. If the resistivity curve exhibits increased resistivity values, it implies the presence of generated hydrocarbons and that the rock is mature. Smagala et al. (1984) noted a good empirical correlation between resistivity and maturity in the Niobrara Formation of the Denver basin. However, in the absence of any correction to the relationship to account for decreasing porosity with depth, it is probably not possible to use their relationship universally.

Effect of Organic Matter Type

No significant dependance on organic matter type (OMT) has been observed when predicting TOC from Δ log R in clay-rich rocks where the TOC values are less

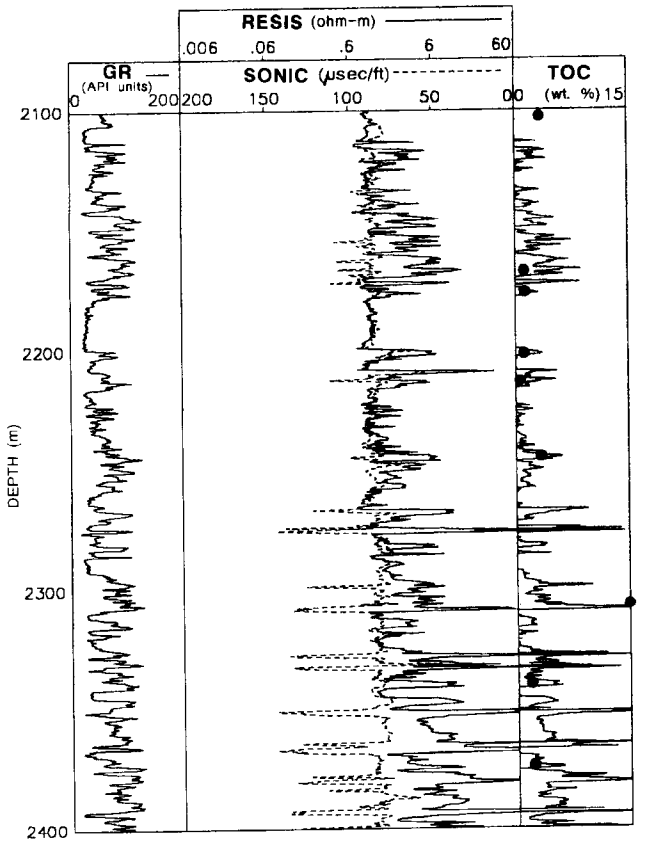

Figure 8—Sonic/resistivity overlay and calculated TOC profile for rocks deposited in a terrigenous environment. Coals are readily apparent from the abrupt sonic "spikes" to higher transit times. Black dots are core data.

than 15 wt. %. However, the proposed calibration is not accurate in predicting TOC values in coals that are clay lean, although the Δ log R technique accurately identifies coals as organic-rich zones.

The technique works well in both oil-prone and gas-prone source rocks. The application of Δ log R to a lacustrine source rock, where the kerogen type is predominately type I (oil-prone), is shown in Figure 7. Note the significant Δ log R separation throughout this interval, and the reasonably good agreement of the calculated TOC values with measured TOC values from sidewall cores.

Because S_2 is a strong function of OMT, the organic matter type must be known in order to calculate meaningful S_2 values from well logs in clay-rich rocks. At the present time, OMT cannot be determined using only well logs, although OMT is easily determined from a few reliable measurements of S_2 of cuttings.

The depositional environment of the organic matter often can be inferred from the vertical distribution of organic matter, and it may be possible to infer expected OMT based on the depositional environment. Coals and coaly sediments are generally more thinly bedded than are the thicker and more continuous marine source rocks. An illustration of how the distribution of TOC may be diagnostic of thinly bedded coals and coaly/deltaic sediments is given in Figure 8. The thinly bedded nature of the sediments is indicated by the numerous high transit-time/high resistivity "spikes" (i.e., alternating organic-rich and organic-poor sediments). The thicker coals could easily be sampled using sidewall cores if one were interested in obtaining maturity data via vitrinite reflectance.

Comparison with Sample Data

Calibration and Accuracy of Calculation of TOC

For many wells, we have been able to directly compare log-derived TOC values with measured TOC values from sidewall cores, conventional cores, or cuttings samples. In most cases the match is very good and has given us confidence to apply the technique in wells for which no samples are available. Also, the ability to perform the Δ log R technique at a well site using properly-scaled sonic and resistivity curves provides an excellent method for identifying organic-rich intervals to be sampled with a sidewall coring tool.

The accuracy of the Δ log R-derived TOC values for organic-rich intervals in six wells with thermal maturities ranging from LOM 6 to LOM 11 is summarized in Table 1. Also included is a comparison with individual well log curves. The well-log and measured TOC data for these

Table 1. Comparison of Accuracy of Predicted Organic Richness

Well	N	LOM	Correlation Coefficient (r^2)						Standard Deviation of Difference (wt. %)
			Δ log R	GR	R_{ild}	ΔT	ρ_b	ϕ_N	
A	24	6–7	.75	.71	.01	.75	.64	.53	±1.4
B	20	7–8	.77	.69	.17	.69	—	—	±1.4
C	10	7	.91	.52	.26	.69	.85	.77	±1.2
D	14	9	.84	.09	.79	.54	—	—	±1.4
E	15	8–9	.88	.45	.59	.39	.26	—	±1.1
F	29	10–11	.47	.56	.40	.01	—	—	±0.9

Correlation coefficients (r^2) are listed for linear relationships between organic richness (TOC) and ΔlogR, and between organic richness and each of several types of log curve data. N is the number of samples analyzed. The standard deviation of the difference refers to the standard deviation of the absolute error (in wt. %) between measured TOC and Δ log R-derived TOC values.

Table 2. Well A (LOM 6–7)

Depth (m)	GR (API)	R_{ild} (ohm-m)	ΔT (μsec/ft)	ρ_b (g/cm³)	ϕ_N	TOC (wt. %)
2249	171	0.93	133	2.13	0.442	9.31
2252	175	0.97	131	2.13	0.398	10.24
2255	195	0.95	132	2.13	0.399	9.59
2262	183	0.79	135	2.07	0.445	8.20
2268	187	0.78	138	2.10	0.410	8.78
2274	181	0.85	132	2.12	0.455	8.47
2278	185	0.59	140	2.10	0.437	9.30
2297	146	0.49	134	2.27	0.351	6.16
2307	153	0.55	133	2.22	0.428	6.32
2313	145	0.77	123	2.18	0.412	5.94
2321	141	0.64	129	2.25	0.430	6.00
2324	150	0.60	130	2.25	0.412	7.04
2329	154	0.65	132	2.20	0.426	9.50
2336	160	0.73	117	2.21	0.419	5.82
2339	159	0.67	130	2.19	0.498	9.49
2342	154	0.68	131	2.19	0.420	7.66
2347	157	0.81	131	2.26	0.384	9.80
2353	156	1.02	136	2.11	0.410	11.30
2362	151	0.77	130	2.24	0.353	7.76
2385	120	1.08	124	2.30	0.367	6.04
2394	116	1.19	116	2.30	0.360	2.42
2414	72	0.97	103	2.35	0.261	1.82
2426	103	0.83	106	2.33	0.278	2.02
2435	99	0.73	104	2.35	0.271	2.80

Table 3. Well B (LOM 7–8)

Depth (m)	GR (API)	R_{ild} (ohm-m)	ΔT (μsec/ft)	ρ_b (g/cm³)	ϕ_N	TOC (wt. %)
2950	145	6.12	126	—	—	9.30
2950	150	3.82	1256	—	—	7.80
2952	172	3.78	1226	—	—	8.75
2953	189	2.90	1096	—	—	6.15
2954	156	2.76	1056	—	—	6.35
2955	168	2.78	1106	—	—	6.85
2956	178	3.51	1216	—	—	10.10
2957	166	3.34	1236	—	—	8.75
2958	159	3.19	1146	—	—	3.25
2964	109	3.49	1086	—	—	5.55
2967	113	3.49	1126	—	—	5.60
2967	107	3.92	1106	—	—	4.28
2967	96	5.34	826	—	—	3.80
2968	67	6.93	736	—	—	3.12
2970	107	2.67	1016	—	—	1.38
2973	75	1.70	886	—	—	0.84
2973	72	1.73	886	—	—	1.73
2974	63	2.07	796	—	—	1.29
2975	65	2.37	906	—	—	1.69
2984	57	1.65	856	—	—	1.15

wells are provided in Tables 2–7.

Correlation coefficients (r^2) are provided to show how the correlation of Δ log R with TOC compares with the correlation of individual well-log curve values with TOC. For organic-rich intervals of low maturity (LOM 6–9) relatively good correlations are noted between TOC and

Table 4. Well C (LOM 7)

Depth (m)	GR (API)	R_{ild} (ohm-m)	ΔT (μsec/ft)	ρ_b (g/cm³)	ϕ_N	TOC (wt. %)
2688	166	4.68	110	2.26	0.354	9.88
2709	158	3.42	109	2.22	0.337	9.10
2729	148	4.57	99	2.27	0.343	8.62
2747	169	2.33	114	2.26	0.351	8.54
2753	179	2.03	115	2.25	0.358	8.18
2771	187	2.96	114	2.25	0.366	9.18
2792	119	2.68	108	2.33	0.311	7.50
2817	126	2.10	94	2.41	0.308	3.82
2827	109	2.58	84	2.43	0.286	3.54
2831	157	3.09	102	2.45	0.309	5.40

Table 5. Well D (LOM 9)

Depth (m)	GR (API)	R_{ild} (ohm-m)	ΔT (μsec/ft)	ρ_b (g/cm³)	ϕ_N	TOC (wt. %)
2090	84	5.77	82	—	—	2.13
2120	60	9.60	68	—	—	0.36
2150	100	8.58	89	—	—	1.51
2155	74	6.94	74	—	—	2.60
2160	78	7.32	75	—	—	2.60
2180	99	4.46	87	—	—	2.57
2190	91	5.48	80	—	—	1.51
2200	98	4.93	83	—	—	1.51
2240	105	10.20	100	—	—	4.16
2245	102	12.64	98	—	—	3.64
2250	114	11.41	104	—	—	4.42
2264	96	39.22	101	—	—	5.19
2270	92	48.51	96	—	—	7.27
2280	88	54.07	99	—	—	8.05

sonic transit time (Δt). The wells of higher maturity (LOM 9–11) exhibit lower correlations with sonic transit time (Δt), but increased correlation with the deep induction resistivity curve (R_{ild}). The correlation with total gamma-ray intensity (GR) varies from good to poor, irrespective of degree of thermal maturity. In all cases, however, the correlation coefficient of TOC with Δ log R is better than that with either of the individual sonic or resistivity curves. As an additional measure of accuracy, Table 1 also contains an absolute error in (wt. %) based on a comparison of the Δ log R-derived TOC values with the measured TOC values. For these six wells, the standard deviation of the difference between calculated and measured TOC values is ±1.4 wt. % or better.

The general calibration of Δ log R to TOC has been confirmed in numerous wells worldwide and for various lithologies. Figure 9 illustrates typical scatter of Δ log R vs. TOC for three of the organic-rich intervals listed in Table 1 (wells A, E, and F).

Vertical Resolution of Thin Source Rock Intervals

Because of the limited vertical resolution of well logs, it is unrealistic to quantify accurately the organic content of source intervals whose thickness is significantly less

Table 6. Well E (LOM 8–9)

Depth (m)	GR (API)	R_{ild} (ohm-m)	ΔT (μsec/ft)	ρ_b (g/cm^3)	ϕ_N	TOC (wt. %)
3322	121	1.59	109	2.45	—	3.42
3325	114	1.76	106	2.37	—	2.42
3337	98	1.77	106	2.38	—	2.98
3355	127	2.25	103	2.43	—	3.04
3365	159	3.03	110	2.40	—	5.32
3367	163	3.66	106	2.44	—	5.40
3380	120	4.80	100	2.47	—	3.86
3385	133	3.80	100	2.47	—	4.90
3410	148	3.45	105	2.44	—	4.50
3418	128	9.37	100	2.46	—	9.45
3422	105	4.32	92	2.51	—	3.74
3429	112	4.84	90	2.49	—	1.99
3445	94	1.86	80	2.65	—	0.14
3452	94	1.80	83	2.52	—	0.06
3456	101	1.92	82	2.63	—	0.38

Table 7. Well F (LOM 10–11)

Depth (m)	GR (API)	R_{ild} (ohm-m)	ΔT (μsec/ft)	ρ_b (g/cm^3)	ϕ_N	TOC (wt. %)
4023	60	1.89	82	—	—	0.26
4035	66	3.35	82	—	—	0.20
4038	58	2.67	70	—	—	0.20
4044	67	1.69	83	—	—	0.22
4048	78	2.49	74	—	—	2.46
4051	118	5.83	108	—	—	1.64
4052	104	4.16	98	—	—	2.84
4054	99	3.65	96	—	—	2.30
4060	115	7.97	86	—	—	1.62
4061	130	10.21	93	—	—	3.58
4063	121	7.92	86	—	—	2.26
4066	118	9.16	92	—	—	2.54
4067	117	9.42	85	—	—	4.12
4069	112	13.54	90	—	—	2.56
4078	140	15.15	84	—	—	2.14
4080	143	15.48	82	—	—	2.96
4081	142	14.23	81	—	—	3.28
4083	169	15.27	77	—	—	2.96
4090	141	15.43	84	—	—	2.76
4092	143	19.09	84	—	—	3.54
4093	135	18.05	81	—	—	2.64
4096	109	12.91	68	—	—	3.04
4098	149	11.86	88	—	—	3.56
4099	141	13.58	82	—	—	2.18
4101	135	8.48	79	—	—	2.96
4102	131	8.36	79	—	—	2.58
4104	136	8.73	77	—	—	2.48
4105	138	8.12	80	—	—	2.32
4107	121	11.33	71	—	—	2.06

than the combined resolution of the porosity/resistivity overlay (approximately 1 m). Source rocks as thin as 0.33 m are readily identified using the sonic/resistivity overlay, but it is unreasonable to expect accurate prediction of TOC in these thin intervals.

Small Δ log R anomalies often occur around thin beds (< 0.5-m thick). These anomalies arise because of differences in the vertical resolution of the resistivity and sonic tools. In practice, these anomalies are insignificant and can be ignored. Initial examination of known thin source intervals with a variety of porosity curves (transit-time, density, and neutron) suggest that none of these curves is significantly better than any other in quantifying the organic richness of thin intervals.

It is necessary to be aware of potential resolution differences and depth misalignments when comparing various sample measurements with log-derived values: whereas the Δ log R-derived TOC values are generally average values over about 1 vertical meter, core data can represent as little as 2.5 cm of borehole depth. Samples are generally of three types: (1) sidewall cores, (2) conventional cores, and (3) cuttings.

Sidewall and Conventional Cores

When a sidewall or conventional core plug is obtained from a largely homogeneous formation, its TOC value should correspond reasonably well to the average TOC values calculated from the well logs. As illustrated in Figure 8, the well logs accurately indicate organic richness in this interval from the Gippsland basin. In thinly bedded formations, however, a single sidewall core or conventional core sample may not agree with the log-derived TOC values at the sidewall core depth.

For example, closely spaced measurements were obtained from a conventional core from the North Sea (Figure 10). Individual measured values may not precisely match the predicted curve, but the overall TOC and S_2 trends and magnitudes are very similar. For the 148 samples presented here, the average log-derived TOC value is 3.01 wt. %, the average measured TOC value is 3.07 wt. %, and the standard deviation of the TOC differences is ±1.2 wt. %.

Cuttings

The quality of the comparison between cuttings-derived data and log-derived TOC values can vary greatly. Variables such as hole quality, sampling rate, drilling rate, and whether or not the cuttings are high-graded for analysis all affect how representative the cuttings are of the true downhole lithology. If the cuttings are collected and analyzed every 3 m or so and the hole is in good condition, then a reasonable agreement is expected between the measured and log-derived TOC values.

A comparison between log-derived S_2 and TOC values and relatively closely spaced cuttings measurements from a well in the Paris basin is shown in Figure 11. For this example, a good agreement is achieved for the thicker source rocks (such as the unit between 2220 and 2285 m), but poorer agreement occurs in the thinner units (such as values between 2150 and 2175 m). The difference between the calculated and measured TOC and S_2 values between 2350 and 2370 m suggests that much of the Δ log R separation in this zone results from reservoired hydrocarbons rather than from kerogen.

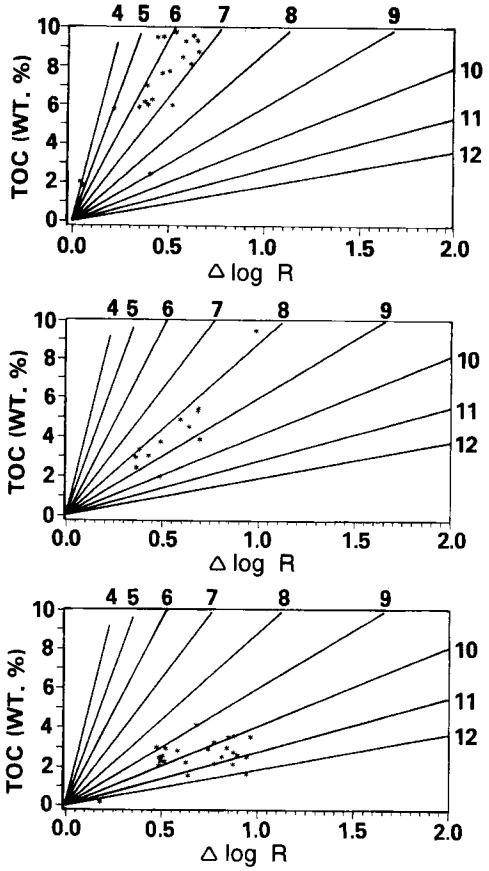

Figure 9—Typical data used to calibrate Δ log R separation to TOC for source rocks of various thermal maturities.

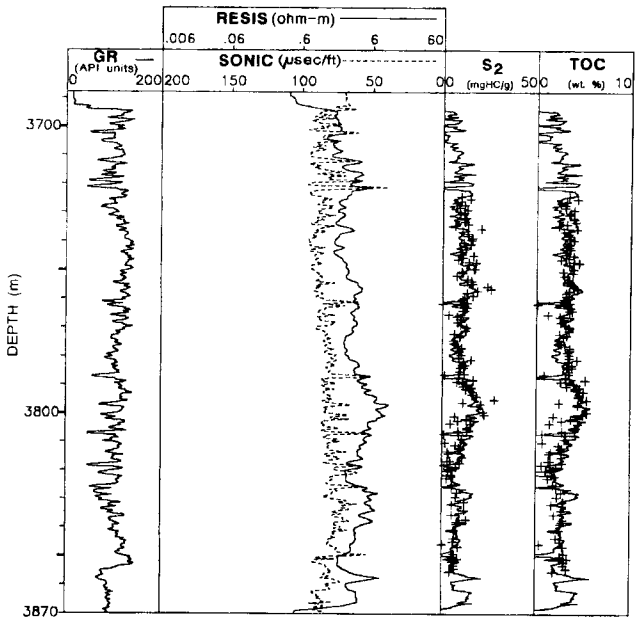

Figure 10—Sonic/resistivity overlay and log-derived S_2 and TOC profiles in an oil-prone marine source rock from the North Sea. The maturity of this interval is LOM 9–10. The abundant measured TOC and S_2 values are from core.

ROUTINE APPLICATION OF THE TECHNIQUE

Interpretation of Δ log R Overlays

The logic used in identifying organic-rich rocks from the various types of porosity/resistivity (Δ log R) separation is illustrated schematically in Figure 12.

The characteristics for organic-rich intervals are illustrated in zones C, F, H, and I. The Δ log R separation in the immature zone C is due entirely from the sonic curve response, whereas, in the mature zone F, the Δ log R separation has both sonic and resistivity curve components. Note that in the coaly sections (zones H and I), the gamma-ray intensity is low. Where coals or coaly sediments are present, they are likely to be thinner and more interbedded than marine organic-rich intervals.

Hydrocarbon reservoirs exhibit a Δ log R separation primarily because of an increase in resistivity due to the non-conductive oil or gas. Typical responses in hydrocarbon reservoirs are shown in zones B, D, and G. Hydrocarbon/water contacts often are readily apparent, as shown in zone G.

Intervals of low porosity have high resistivities because of an absence of electrically conducting fluid, as shown in zone K. These intervals can be recognized by relatively short transit times (generally less than 180 μsec/m or 55 μsec/ft).

Intervals of non-source or non-reservoir generally have porosity and resistivity curves overlying (i.e., baselined), as shown in zones A, E, and J.

Anomalous Δ log R Separation

Anomalous Δ log R separation not associated with source intervals generally can be attributed to (1) hydrocarbon reservoirs, (2) poor borehole conditions, (3) uncompacted sediments, (4) low-porosity (tight) intervals, (5) volcanics, or (6) evaporites.

Reservoir Intervals

In hydrocarbon-bearing reservoirs, a Δ log R separation generally is observed. Figure 13 illustrates this condition in a gas reservoir (4400–4480 m) immediately beneath a mature source interval (4340–4380 m). The gamma-ray curve can be used to differentiate the reservoir zone from the source interval. In practice, when baselined in shales, the sonic porosity curve in reservoirs generally moves to the right (shorter transit times), as shown in Figure 12, zone B, or may exhibit no change, as shown in Figure 12, zone D. If the porosity is high in the reservoir zone, the transit-time curve can move to the left (zone G); this case is not common, but can be confused with organic-rich intervals if the gamma-ray curve is not diagnostic.

Although reservoirs generally can be distinguished from organic-rich rocks by low gamma-ray intensities, the gamma-ray intensity can be high in some instances, as is observed in reservoirs consisting of feldspar or mica-rich

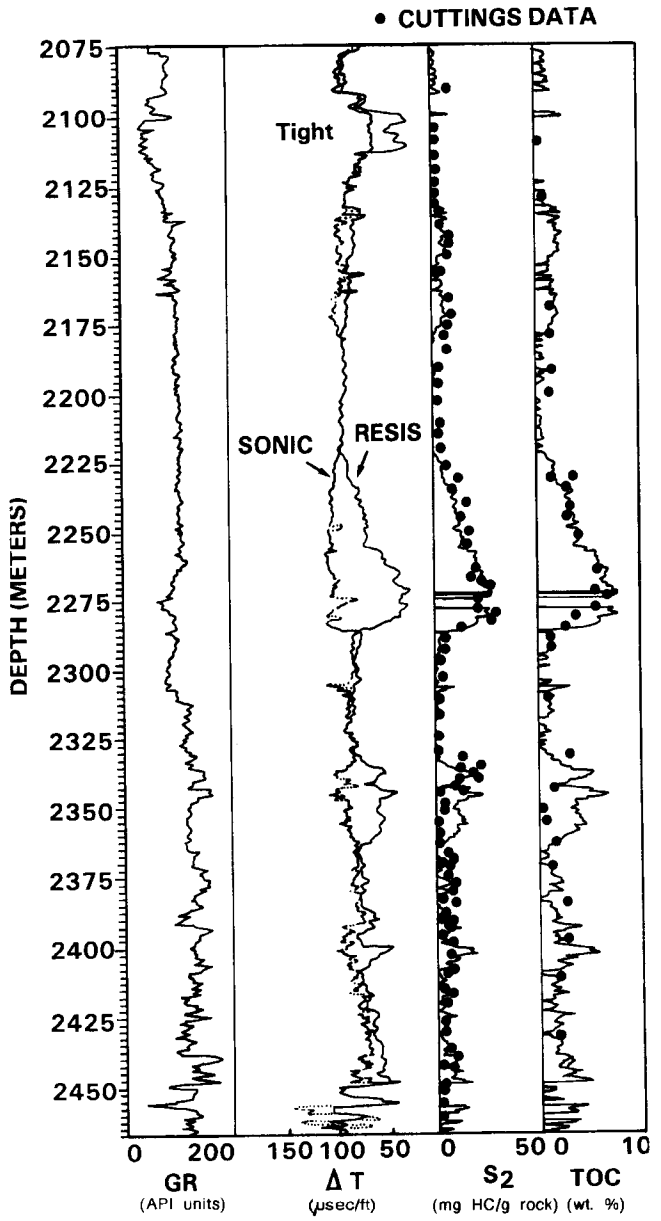

Figure 11—Comparison between log-derived S_2 and TOC values and cuttings-measured values (black dots) for a well in the Paris basin. Because of a change in lithology at 2285 m, a shift in the baseline was necessary. For this reason, no resistivity scale is shown. Above 2285 m, $R_{baseline}$ is 2.4 ohm-m; below 2285 m, $R_{baseline}$ is 1.0 ohm-m.

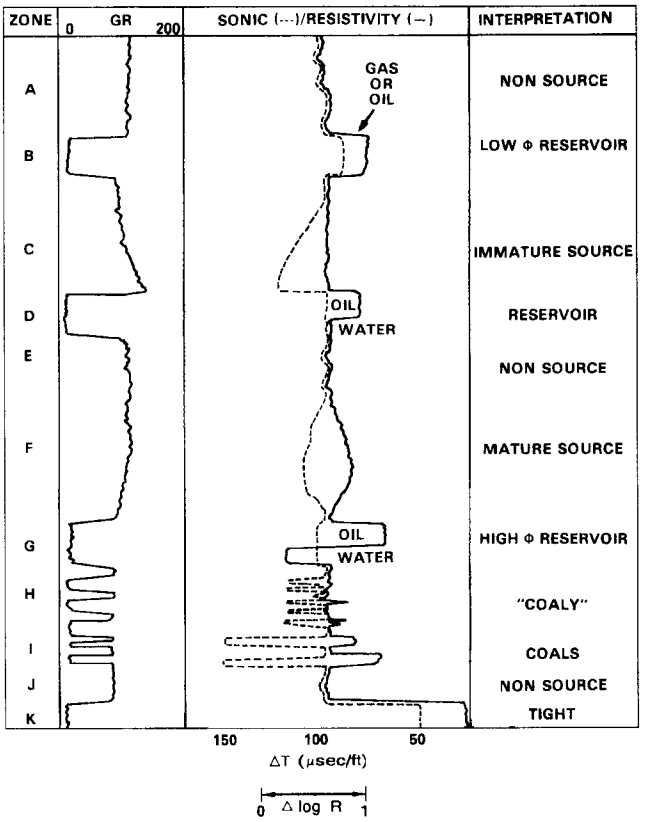

Figure 12—Schematic guide for the interpretation of a wide variety of features observed on Δ log R overlays.

sandstones. An example of a radioactive reservoir sandstone is shown in Figure 14. Although the reservoir interval displays higher gamma-ray values than expected, the absence of higher transit times (i.e., the TOC component) in the Δ log R separation reflects the absence of solid organic matter. In such cases, routine log analysis techniques, such as a density/neutron crossplot or overlay, can be useful in distinguishing clay-rich intervals from clay-lean intervals. Three small possible organic-rich intervals are identified between 980 and 1100 m.

Poor Borehole

Poor boreholes often are indicated by large washouts, and most logging tools will not read accurately if the washouts are too severe. Examination of the caliper log is essential if excessively numerous zones of Δ log R separation are observed, or if no intervals of good tracking are observed on which to establish a baseline. Cycle skipping is often observed on the transit-time curve in poor boreholes, and these cycle skips should not be interpreted as thin coals; generally, the transit times of the cycle skips exceeds the transit times for coals. When the transit times exceed about 150 μsec/ft (500 μsec/m), the Δ log R separation should not be relied upon to predict organic richness.

Uncompacted Sediments

In uncompacted sediments, correspondence between resistivity and sonic curves is poor, with transit times much longer than accounted for by the resistivity curve. In relatively young, shallow, uncompacted rocks, the shale transit times often exceed 150 μsec/ft (500 μsec/m), and any Δ log R separation observed in these intervals may be misleading. Thus, one should exercise caution in interpreting any Δ log R separation in relatively young, shallow, uncompacted sediments.

Low Porosity (Tight) Intervals

When the porosity of the formation is less than 3–4%, the resistivity increases greatly because of a lack of elec-

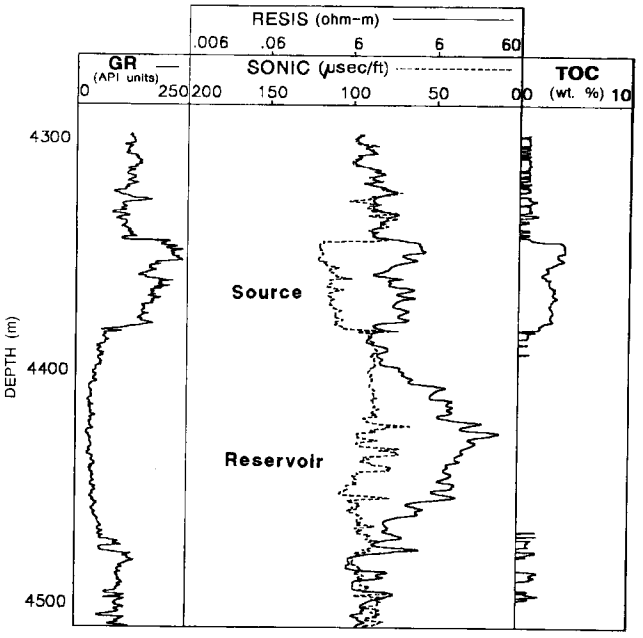

Figure 13—Sonic/resistivity overlay and calculated TOC profile in an interval containing both a source rock and a gas-bearing reservoir. A gamma-ray cutoff was used to exclude the reservoir interval from the TOC-calculation procedure.

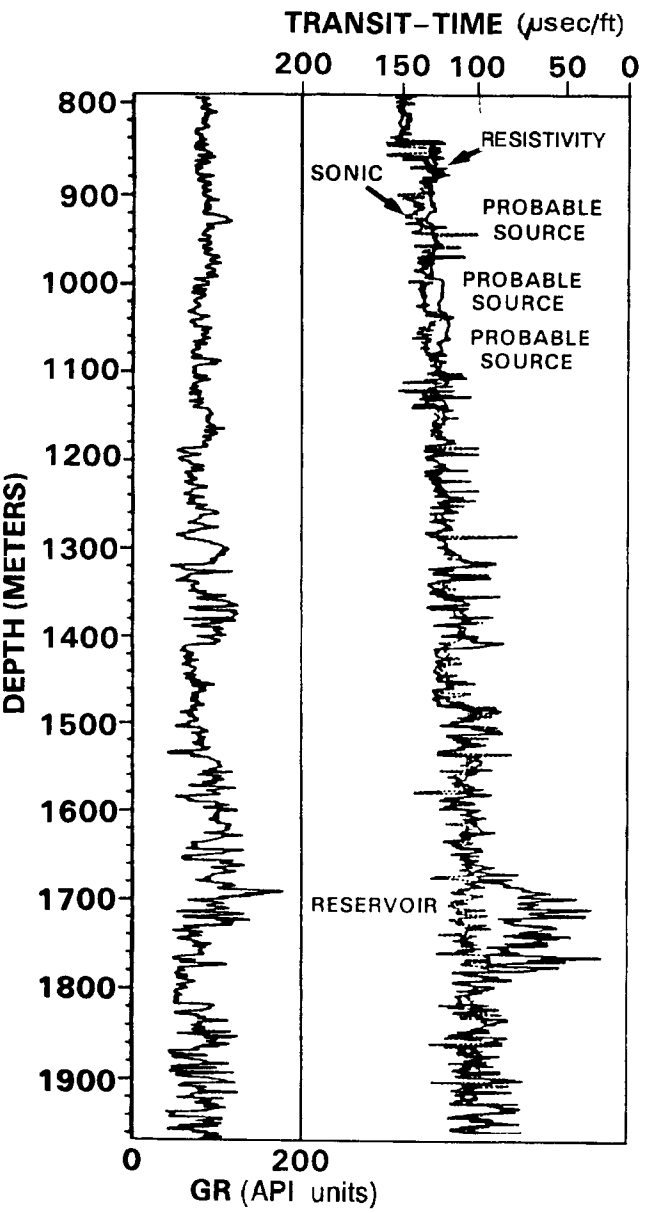

Figure 14—Sonic/resistivity overlay in a section containing both source and reservoir intervals. Because of the presence of radioactive minerals in the reservoir interval, the gamma-ray curve is not useful in identifying reservoirs. For this example, $R_{baseline}$ = 2 ohm-m.

trically conducting fluid. In these low-porosity (tight) intervals, the Δ log R separation often is very large (refer to the Appendix for a discussion of the physical reasons). However, these low-porosity intervals are easily identified by their relatively short transit times (generally 50–55 μsec/ft, 164–180 μsec/m). Typical Δ log R separation in several low-porosity (tight) intervals is illustrated in Figure 15. For the low-porosity (tight) zones, the Δ log R separation is due almost entirely to the resistivity curve response. Note the contrasting Δ log R response within the organic-rich source interval between X520 and X555 m, where the transit-time curve moves to higher values.

Igneous Rocks

Igneous rocks, both intrusive (e.g., sills, laccoliths, etc.) and extrusive (e.g., lava flows, pyroclastic flows, etc.) generally exhibit anomalous Δ log R separation. The gamma-ray intensity of these intervals can be either high or low, depending on the mineralogy, but all generally exhibit relatively low transit-time values, typically near 50 μsec/ft (164 μsec/m) and high resistivity. These igneous zones appear similar to the low-porosity (tight) intervals previously discussed and, as before, the key for correct interpretation is noting a lack of TOC response in the porosity component of the Δ log R response.

Evaporites

In massive salt intervals, the resistivity generally is very high, leading to a large anomalous Δ log R separation. However, they can be easily distinguished by a nearly constant transit time of 67.5 μsec/ft (221 μsec/m), associated with low gamma-ray intensities. An example of typical anomalous Δ log R separation in massive salt beds is given in Figure 16. In addition, two possible organic-rich source intervals are identified by their Δ log R separation, as well as a water zone exhibiting negative separation.

Overpressured Zones

In overpressured zones, the observed porosity exceeds the expected porosity. Baselining the transit-time and resistivity curves roughly compensates for this increased porosity; thus, no significant anomalous Δ log R separa-

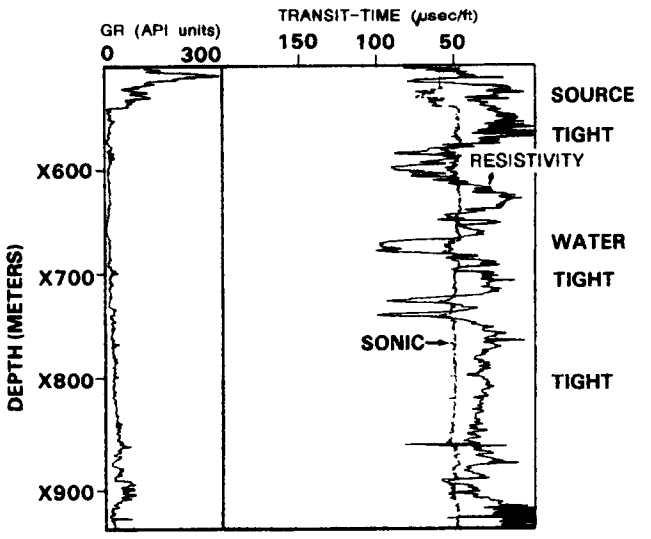

Figure 15—Low-porosity intervals showing anomalous Δ log R separation. Note that the transit-time curve reads approximately 50 μsec/ft (164 μsec/m), indicating low porosity. For this example $R_{baseline}$ = 12 ohm-m.

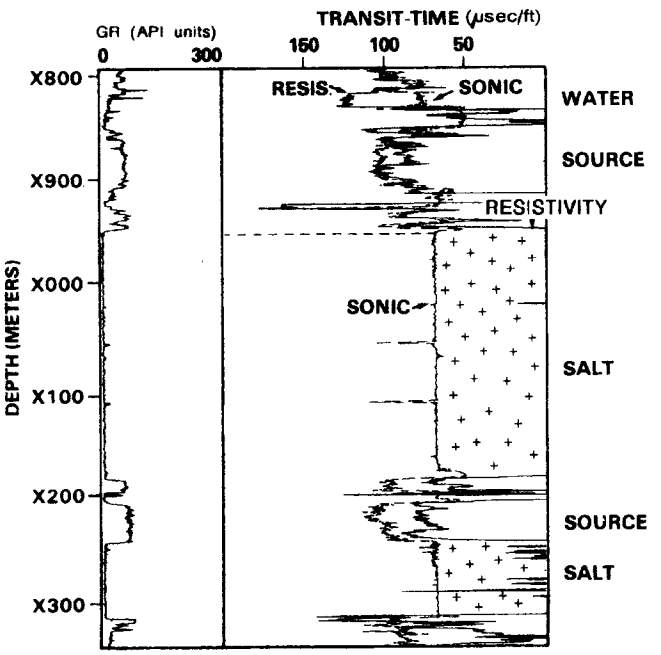

Figure 16—Massive salt exhibiting anomalous Δ log R separation with possible organic-rich intervals between the salt beds. For this example, $R_{baseline}$ = 2 ohm-m.

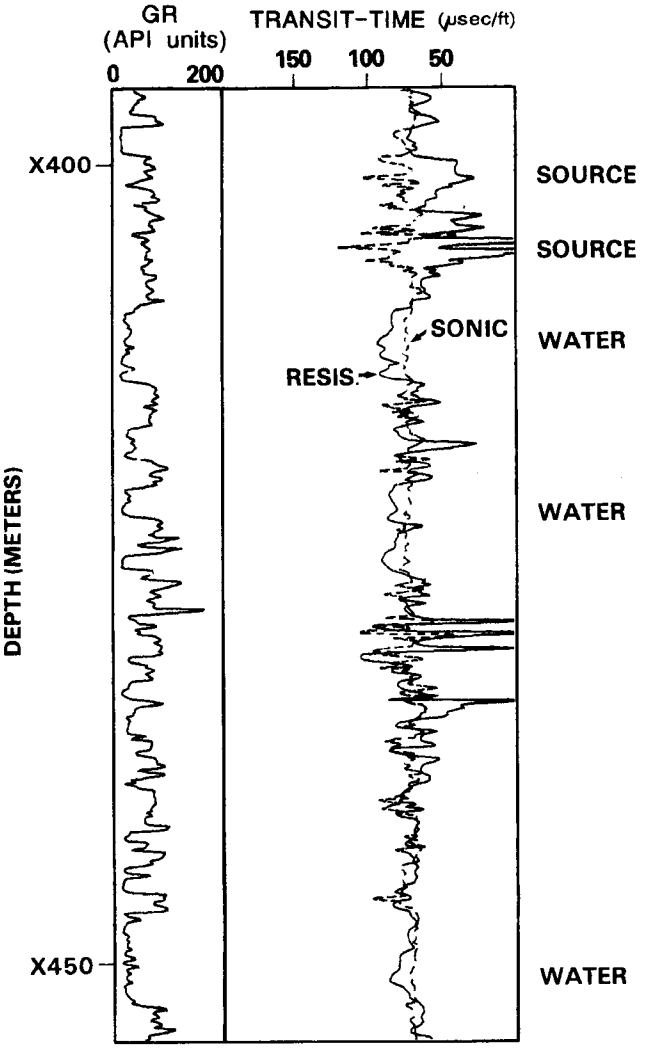

Figure 17—Sonic/resistivity overlay showing negative separation (i.e., the resistivity curve to the left of the sonic curve) in saline water-filled sandstones (when baselined in shales). For this example, $R_{baseline}$ = 4 ohm-m.

tion occurs within the overpressured zone unless the zone is organic-rich or a hydrocarbon reservoir.

Water-filled Porous Intervals

Intervals that are largely sand dominated often exhibit negative separation (where the resistivity curve is to the left of the porosity curve on the Δ log R plot) in the water-filled sandstones when the curves are baselined in shale lithologies (Figure 12, lower part of zone G). Strong negative separation in sands probably reflects higher salinity formation fluids in the sandstones compared to those of the shales. This is particularly evident in coastal plain facies. An example of negative separation in saline-water filled sandstones is illustrated in Figure 17. In this example the negative separation in the sandstones should be ignored, and the shales can be evaluated as usual for potential organic-rich intervals. A potential organic-rich source interval is shown between X400 and X410 m.

Finally, it should be stressed that a single baseline generally cannot be defined for an entire well because of variable lithology and/or changes in formation water salinity. Generally a baseline shift occurs at carbonate/clastic interfaces and where formation water salinities change drastically. Also, gradual baseline shifts are necessary to

account for compaction with depth. In these cases, each unit must be baselined separately, and the results integrated into the final well profile of calculated TOC values. To provide a continuous overlay that is useful in identifying unconformities as well as source rocks, it is preferred to shift the resistivity curve rather than the transit-time curve, thus maintaining an unmodified compaction curve that is useful in interpreting unconformities as well as lithology and overpressure.

CONCLUSIONS

(1) The Δ log R technique uses common, widely available well logs to identify organic-rich source rocks and to calculate their TOC content.

(2) The Δ log R separation displayed by properly scaled transit-time and resistivity curves can be used to determine accurately organic richness with a vertical resolution of about 1 m. Other porosity curves (e.g. density and neutron) can be substituted for the transit-time curve, if necessary, but because of borehole compensation, the transit-time curve is preferred.

(3) Thin organic-rich rocks (less than 0.5 m thick) can be detected using the Δ log R technique, but the calculated TOC values are likely to be lower than measured values based on a routine core plug.

(4) For rocks of low thermal maturity, the relationship between Δ log R and TOC exists primarily because of the porosity curve component of Δ log R. As maturity increases, the resistivity curve component becomes increasingly important. Although source rocks from LOM 5 to LOM 15 have been evaluated using the Δ log R technique, the calibration is applicable primarily between LOM 7 (onset of oil generation) and LOM 12 (onset of overmaturity). For maturities below LOM 6 or above LOM 12, the relationships for LOM 6 and 12 generally are applied, but the calibration is not rigorous at these extremes.

(5) The empirical relationship between Δ log R separation and TOC is the primary relationship, and the relationship of Δ log R to organic matter type (S_2) is secondary.

(6) Δ log R separation not associated with organic-rich source rocks can occur but, in most cases, such anomalous Δ log R intervals can be easily recognized and disregarded. The primary pitfalls include (a) hydrocarbon reservoirs, (b) poor borehole conditions, (c) uncompacted sediments, (d) low porosity (tight) intervals, (e) igneous rocks, and (f) evaporites.

APPENDIX: THEORETICAL RESISTIVITY/TRANSIT-TIME RELATIONSHIPS

To understand better how lithology might affect the application of the technique, some theoretical considerations are presented. Of specific interest is the applicability of the relative scaling of the logarithmic resistivity and sonic curves used to baseline the curves in water-filled non-organic-rich shales (i.e., one cycle of resistivity corresponds to −50 μsec/ft or −164 μsec/m). A comparison between the theoretical results from these models and empirical observations confirms the validity of the approach presented in the text.

The Archie equation relating resistivity to porosity is

$$R_t = (R_w\, a)/(S_w^n\, \phi^m) \qquad \text{(A-1)}$$

where R_t is the true formation resistivity, R_w is the resistivity of the formation water, a is a constant (generally assumed to be 1), S_w is the water saturation, n is the saturation exponent, ϕ is the fractional porosity, and m is the cementation exponent (after Archie, 1942).

Assuming that a = 1 and that within a water zone $S_w = 1$, equation (A-1) reduces to

$$R_o = R_w/\phi^m \qquad \text{(A-2)}$$

where R_o is the formation resistivity in a water-saturated zone.

Several relationships exist that relate sonic transit time to porosity. In this paper, two relationships are discussed. One relationship is the well-known Wyllie time-average equation:

$$\phi = (\Delta t - \Delta t_m)/(\Delta t_f - \Delta t_m) \qquad \text{(A-3)}$$

where Δt is the measured sonic transit time in μsec/ft, Δt_m is the matrix transit time, and Δt_f is the fluid transit time (Wyllie et al., 1958).

For non-shale lithologies, substituting ϕ from the Archie equation into the Wyllie equation (A-3) results in

$$R_o = R_w / ((\Delta t - \Delta t_m)/(\Delta tf - \Delta t_m))^m . \qquad \text{(A-4)}$$

Taking the logarithm of equation (A-4) results in

$$\log_{10}(Ro) = \log_{10}((R_w/((\Delta t - \Delta t_m)/\Delta t_f - \Delta t_m)^m) . \qquad \text{(A-5)}$$

Using equation (A-5), it is possible to construct a crossplot of theoretical logarithmic resistivity versus linear transit time for sandstone, limestone, and dolomite (Figure 18). For each lithology, m = 2 and the formation fluid is assumed to be water with $R_w = 0.1$ ohm-m and Δt_f = 189 μsec/ft (620 μsec/m). For sandstone, the matrix transit time Δt_m is assumed to be 55.5 μsec/ft (182 μsec/m); for limestone, Δt_m is assumed to be 47.6 μsec/ft (156 μsec/m); and for dolomite, Δt_m is assumed to be 43.5 μsec/ft (143 μsec/m) (Schlumberger, 1987).

Another sonic porosity relationship was proposed specifically for shales (Magara, 1978). This empirical relationship, derived from organic-lean Cretaceous shales within the Alberta basin, has the form

$$\phi = (0.00466\,\Delta t - 0.317)^m \qquad \text{(A-6)}$$

where Δt is measured in μsec/ft. Although this empirical relationship is not universal for all shales, the shale porosities obtained using it are more accurate than shale porosities predicted using the Wyllie time-average equation.

As before, combining the Archie equation (A-2) with the shale porosity equation (A-6) results in

$$R_o = R_w/(0.00466\,\Delta t - 0.317)^m . \qquad \text{(A-7)}$$

Taking the logarithm of equation (A-7) results in

$$\log_{10}(R_o) = \log_{10}((R_w/0.00466\,\Delta t - 0.317)^m) . \qquad \text{(A-8)}$$

Using equation (A-8), a shale line can be constructed assuming m = 2 and $R_w = 0.1$ ohm-m (Figure 18). Note that the trends for all lithologies shown on Figure 18 are nonlinear. For any given transit time, the theoretical slope of the curve can be obtained by differentiation of equations (A-5) and (A-8).

The zone for which the nonlinear curves can be approximated by a linear slope of −1:50 (for μsec/ft) is bounded by the heavy solid lines. Within this zone, the curve baseline parameters in equation (1) (i.e., $\Delta t_{baseline}$ and $R_{baseline}$) constitute an ordinate pair for such a line with a slope of −1:50 (e.g., $\Delta t_{baseline}$ = 100 μsec/ft and $R_{baseline}$ = 1.0 ohm-m).

For shales, this zone corresponds to transit times between 80 μsec/ft (262 μsec/m) and 140 μsec/ft (460 μsec/m). Within this zone, errors in calculated TOC values associated with the −1:50 (for μsec/ft) slope approximation are small. Erroneous TOC calculation using the Δ log R technique

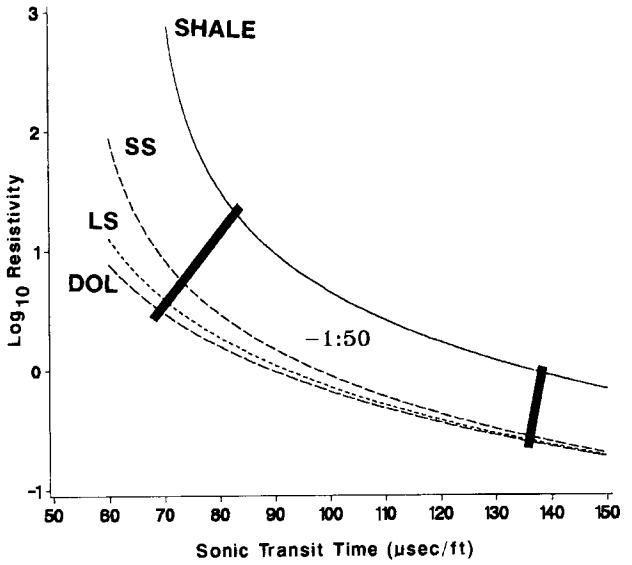

Figure 18—Comparison of theoretical relationships between logarithmic resistivity and transit time for four different lithologies. The form of the shale curve differs slightly from the other curves primarily because a different equation relating porosity to transit time was used. The heavy lines mark boundaries of the zone for which the –1:50 relative scaling of the sonic (in μsec/ft) and logarithmic resistivity curves can be applied. Although these curves were constructed assuming a formation water resistivity (R_w) of 0.1 ohm-m, the slopes of the lines at specific transit times are the same for other values of R_w.

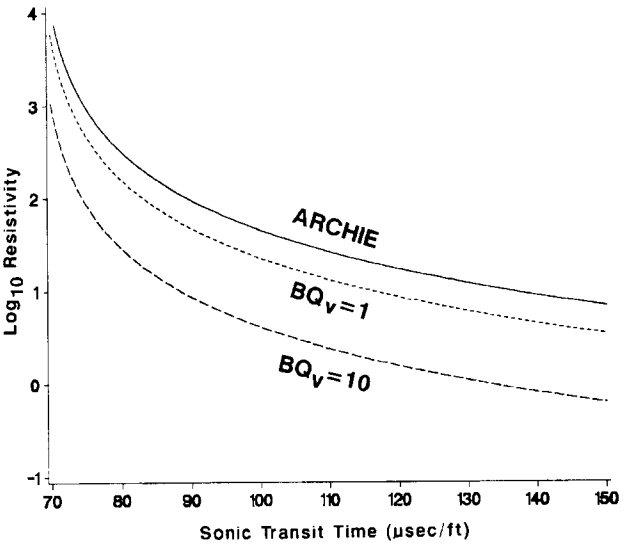

Figure 19—Comparison of theoretical results derived from the Archie equation with those from the Waxman-Smits equation (assuming BQ_v = 1 and BQ_v = 10). These curves were constructed assuming that R_w = 1 ohm-m.

is expected at extreme high or low transit times, because the –1:50 slope is not valid. As discussed in the text, potential pitfalls occur for intervals of both low porosity (short transit times) and high transit time (uncompacted sediments). Both of these extremes are easily recognized, and generally neither is associated with present-day mature source rocks (i.e., shales with these transit times are either overmature or immature, respectively). Although the –1:50 relative scaling for the logarithmic resistivity and sonic curves (in μsec/ft) is only an approximation, this scaling has been found applicable to a wide range of lithologies and transit times.

As shown in Figure 18, for a given water resistivity and transit time, the predicted resistivity for the shale is higher than for the other lithologies. This can be explained by realizing that for a given transit time, the shale porosity usually is much less than the porosities for the other lithologies; also, this figure is constructed using the Archie relationship, which does not take into account any additional clay conductivity that might be present.

As this paper is concerned largely with source shales, it is important to consider the theoretical porosity-resistivity relationship for shales where excess conductivity arises from the presence of clay minerals. Specifically, we are concerned if the presence of clay conductivity significantly affects the slope of the relationship between the logarithmic resistivity and linear sonic transit time. For this discussion, the Waxman-Smits (1968) equation is used to model the clay conductivity effects. This equation can be written as

$$1/R_t = (S_w^{n^*}\,\phi^{m^*}/R_w) + BQ_v\,S_w^{(n^*-1)}\phi^{m^*} \qquad \text{(A-9)}$$

where BQv is the term arising from clay conductivity, ϕ is the fractional porosity, R_t is the true resistivity of the formation, S_w is the water saturation, R_w is the formation water resistivity, and m* and n* are the corresponding exponents. Again, for the water-bearing zone, S_w = 1, and equation (A-9) reduces to

$$R_o = (R_w/(\phi^{m^*}(1 + R_wBQ_v)). \qquad \text{(A-10)}$$

Substituting the relationship for shale porosity given by equation (A-6) into equation (A-10) and taking the logarithm results in

$$\log\ (R_o) = \log\,(R_w/((.00466\Delta t - 0.317)^{m^*}\,(1 + R_wBQ_v)). \qquad \text{(A-11)}$$

Figure 19 shows a comparison of the relationship between log (R_o) and transit time for the Archie relation (BQ_v = 0) and the Waxman-Smits equation (BQ_v = 1 and BQ_v = 10). As expected, the Waxman-Smits relation gives a lower resistivity due to the clay conductivity; however, the slope of the log (resistivity)–transit time relationship is not strongly affected by the excess conductivity. Thus, if excess clay conductivity exists in the shale, the relative scaling of the resistivity and porosity curves is unaffected, and the process of baselining the curves removes any difference due to clay conductivity.

REFERENCES CITED

Abrahao, D., 1989, Well log evaluation of lacustrine source rocks of the Lagoa Feia Formation, Lower Cretaceous, Campos basin, offshore Brazil: Transactions of the Thirteith SPWLA Annual Logging Symposium, paper I.

Archie, G. E., 1942, The electrical resistivity log as an aid in determining some reservoir characteristics: Society of Petroleum Engineers of AIME Transactions, v. 146, p. 54–62.

Autric, A., and P. Dumesnil, 1984, Les diagraphies de resistivite, radioactivite et temps de transit (Ts) evaluent le contenu en matieres organiques des roches a faible permeabilite: Societe pour l'Avancement de l'Interpretation des Diagraphies, Ninth International Formation Evaluation Transactions, paper 40.

Autric, A., and P. Dumesnil, 1985, Resistivity, radioactivity and sonic transit time logs to evaluate the organic content of low permeability rocks: The Log Analyst, v. 26, p. 36–45.

Beers, R. F., 1945, Radioactivity and organic content of some paleozoic shales: AAPG Bulletin, v. 29, p. 1–22.

Dellenbach, J., J. Espitalie, and F. Lebreton, 1983, Source rock logging: Transactions of the 8th European SPWLA Symposium, paper D.

Espitalie, J., M. Madec, and B. Tissot, 1977, Source rock characterization method for petroleum exploration: 9th Annual Offshore Technology Conference, p. 439–448.

Fertl, W. H., and H. H. Rieke, 1980, Gamma-ray spectral evaluation techniques identify fractured shale reservoirs and source-rock characteristics: Journal of Petroleum Technology, v. 31, p. 2053–2062.

Flower, J. G., 1983, Use of sonic-shear-wave/resistivity overlay as a quick-look method for identifying potential pay zones in the Ohio (Devonian) Shale: Journal of Petroleum Technology, March, p. 638–642.

Herron, S. L., 1986, Derivation of a total organic carbon log for source rock evaluation: Transactions of the Twenty-Seventh SPWLA Annual Logging Symposium, paper HH.

Herron, S. L., L. Letendre, and M. Dufour, 1988, Source rock evaluation using geochemical information from wireline logs and cores (abs.), AAPG Bulletin, v. 72, p. 1007.

Hood A., C. C. M. Gutjahr, and R. L. Heacock, 1975, Organic metamorphism and the generation of petroleum: AAPG Bulletin, v. 59, p. 986–996.

Lawrence, T. D., S. Ball., and M. Harris, 1984, Continuous carbon/oxygen and neutron lifetime log proposed interpretation for organic and/or shaly depositional environments: Transactions of the Twenty-Fifth SPWLA Annual Logging Symposium, paper QQ.

Magara, K., 1978, Compaction and fluid migration: New York, Elsevier Scientific, 319 p.

Mann, U., and P. J. Muller, 1988, Source rock evaluation by well log analysis (Lower Toarcian, Hils Syncline): Advances in Organic Geochemistry 1987, v. 13, p. 109–119.

Mann, U., D. Leythaeuser, and P. J. Muller, 1986, Relation between source rock properties and wireline log parameters. An example from Lower Jurassic Posidonia Shale, NW Germany: Advances in Organic Geochemistry 1985, v. 10, p. 1105–1112.

Meissner, F. F., 1978, Petroleum geology of the Bakken Formation Williston basin, North Dakota and Montana, *in* The economic geology of the Williston basin: Montana Geological Society, 1978 Williston Basin Symposium, p. 207–227.

Mendelson, J. D., 1985, Petroleum source rock logging, Master's thesis, Massachusetts Institute of Technology, Cambridge, Massachusetts, 93 p.

Mendelson, J. D., and M. N. Toksoz, 1985, Source rock characterization using multivariate analysis of log data, Transactions of the Twenty-Sixth SPWLA Annual Logging Symposium, paper UU.

Meyer, B. L., and M. H. Nederlof, 1984, Identification of source rocks on wireline logs by density/resistivity and sonic transit time/resistivity crossplots: AAPG Bulletin v. 68, p. 121–129.

Murray, G. H., 1968, Quantitative fracture study—Sanish pool, McKenzie County, North Dakota: AAPG Bulletin v. 52, p. 57–65.

Nixon, R. P., 1973, Oil source beds in Cretaceous Mowry Shale of northwestern interior United States: AAPG Bulletin, v. 57, p. 136-161.

Passey, Q. R., S. Creaney, J. B. Kulla, F. J. Moretti, and J. D. Stroud, 1989, Well log evaluation of organic-rich rocks, 14th International Meeting on Organic Geochemistry, Paris, abstract 75.

Philippi, G. T., 1968, On the depth, time, and mechanism of petroleum generation: Geochimica et Cosmochimica Acta, v. 29, p. 1021–1049.

Rieke, H. H., III, D. W. Oliver, W. H. Fertl, and J. P. McCord, 1980, Successful application of carbon/oxygen logging to coalbed exploration, 55th Annual Fall Technical Conference of the Society of Petroleum Engineers, Dallas, Texas, September 21-24, 1980.

Schlumberger, 1987, Log interpretation principles/applications: Houston, Schlumberger Educational Services, 198 p.

Schmoker, J. W., 1979, Determination of organic content of Appalachian Devonian shales from formation-density logs: AAPG Bulletin, v. 63, p. 1504–1537.

Schmoker, J. W., 1981, Determination of organic-matter content of Appalachian Devonian shales from gamma-ray logs: AAPG Bulletin, v. 65, p. 1285–1298.

Schmoker, J. W., and T. C. Hester, 1983, Organic carbon in Bakken Formation, United States portion of Williston basin: AAPG Bulletin, v. 67, p. 2165–2174.

Schmoker, J. W., and T. C. Hester, 1989, Oil generation inferred from formation resistivity—Bakken Formation, Williston basin, North Dakota: Transactions of the Thirtieth SPWLA Annual Logging Symposium, paper H.

Sinclair, I. K., 1988, Evaluation of Mesozoic-Cenozoic sedimentary basins in the Grand Banks area of Newfoundland and comparison with Falvey's (1974) rift model: Bulletin of Canadian Petroleum Geology, v. 36, p. 255–273.

Smagala, T. M., C. A. Brown, and G. L. Nydegger, 1984, Log-derived indicator of thermal maturity Niobrara Formation, Denver Basin, Colorado, Nebraska, Wyoming, *in* J. Woodward, F. F. Meissner, and J. L. Clayton eds., Hydrocarbon source rocks of the greater Rocky Mountain region: Rocky Mountain Association of Geologists, p. 355–363.

Supernaw, I. R. , D. M. Arnold, and A. J. Link, 1978, Method for in-situ evaluation of the source rock potential of earth formations: United States Patent 4,071,744, January 31, 1978.

Swanson, V. E., 1960, Oil yield and uranium content of black shales: USGS Professional Paper 356-A, p. 1–44.

Tannenbaum, E., and Z. Aizenshtat, 1985, Formation of immature asphalt from organic-rich carbonate rocks—I, geochemical correlation: Organic Geochemistry, v. 8, p. 181–192.

Tissot, B. P., and D. H. Welte, 1984, Petroleum formation and occurrence: New York, Springer-Verlag, 699 p.

Waxman, M. H., and L. J. M. Smits, 1968, Electrical conductivities in oil-bearing shaly sands: Society of Petroleum Engineering Journal, June 1968, p. 107–122.

Wyllie, M. R. J., A. R. Gregory, and G. H. F. Gardner, 1958, An experimental investigation of factors affecting elastic wave velocities in porous media: Geophysics, v. 23, p. 459.